



# Subsurface warming derived by Argo floats during the 2022 Mediterranean marine heatwave

Annunziata Pirro<sup>1</sup>, Riccardo Martellucci<sup>1</sup>, Antonella Gallo<sup>1</sup>, Elisabeth Kubin<sup>1</sup>, Elena Mauri<sup>1</sup>, Mélanie Juza<sup>2</sup>, Giulio Notarstefano<sup>1</sup>, Massimo Pacciaroni<sup>1</sup>, Antonio Bussani<sup>1</sup>, Milena Menna<sup>1</sup>

5

<sup>1</sup>National Institute of Oceanography and Applied Geophysics (OGS), Trieste, 34010, Italy

<sup>2</sup>Laboratory Balearic Islands Coastal Observing and Forecasting System (SOCIB), Palma, 07122, Spain

*Correspondence to:* Annunziata Pirro (apirro@ogs.it)

## Abstract.

10 The Mediterranean marine heatwave during the warm season (May-September) and the fall period (October-December) of 2022 is analysed using Argo floats in-situ observations in the upper 2000 m of depth. Based on the 2022 ocean heat content anomaly, five study regions (North Western Mediterranean, South Western Mediterranean, central Ionian Sea, Pelops Gyre, southern Adriatic Sea) most affected by warming in different layers were selected and investigated. Temperature anomaly profiles  $T'(z)$  computed for each area and for both periods, were divided into three categories based on vertical heat penetration:

15 Category 1 (shallow, 0-150 m), Category 2 (intermediate, 150-700 m) and Category 3 (deep, > 700 m). Category 1 profiles had a temperature anomaly near zero or slightly negative in a thin layer between 50 m and 150 m depth, while warming was observed below the middle layer. Profiles characterized by greater vertical heat penetration (categories 2 and 3) were mainly in mesoscale or sub basin structures and showed the largest positive temperature anomaly in the surface layer and thermocline. All profile categories showed warming between 200 and 800 m depth. During the fall period all sectors show similar warming

20 in the layer below 200 m depth, except for the SAP, which records an anomalous warming in the intermediate and deep layer. The present work highlights the warming characteristics along the entire water column in different regions of the Mediterranean Sea, some of which are characterized by dynamic activities. This sheds light on possible scenarios changes with implications on the variation of the ocean processes that regulate the thermohaline circulation and thus, the climate system.

25

## Introduction

Marine heatwaves (MHWs) are extreme ocean temperature events occurring over extended periods of time (Hobday et al., 2016). Over the past decade MHWs have increased worldwide their frequency by 50% (IPCC, 2023) as well as their duration and magnitude (Oliver et al., 2018). They can affect small areas of coastline or span multiple ocean areas across latitudes with



30 significant impacts on ecosystems, coastal communities and economies (Wernberg et al., 2013; Garrabou et al., 2022; Dayan et al., 2023).

Since the beginning of the 21<sup>st</sup> century the particularly rapid warming trend of the Mediterranean Sea surface layer has been associated with a strong increase in MHWs (Bensoussan et al., 2019, Ibrahim et al, 2021, Juza et al., 2022, Pastor and Khodayar, 2022, Dayan et al., 2023). Several studies, mainly confined at the surface, have addressed this topic facing different  
35 aspects of MHWs using satellite observations and model simulations. In particular, from basin to sub-regional scale, previous works analyse MHWs drivers and indicators, estimate the frequency, the duration and intensity of MHWs, evaluate their trend and assess the risk and the impacts on ecosystems (Dayan et al., 2022, Darmaraki et al 2019, Galli et al., 2017, Garrabou et al., 2022, Juza et al., 2022, among others).

40 However, MHWs are not exclusively limited to the surface layer, but they can also propagate throughout the deeper layers of the water column (Darmaraki et al., 2019, Shijian et al., 2021, Scannell H.A., 2020, Juza et al., 2022). A recent work in the Mediterranean Sea shows that although MHWs frequency is higher at the surface, their maximum intensity and duration is registered in the subsurface layers (Dayan et al., 2023). Moreover, in-situ data collected in the tropical western Pacific Ocean show that the maximum intensity of almost every MHW event is found in the subsurface layer, and many of the MHWs  
45 occurred even when no significant warming anomalies are detected at the surface (Shijian et al., 2021).

The present work analyses the subsurface properties of the 2022 MHW in the upper 2000 m depth using in-situ hydrographic Argo profiles (Product ref. no. 1, Table 1; Wong et al., 2020) collected during the event (May-September 2022) and after the event (October-December 2022) in the Mediterranean Sea (Figure 1(b)). Focusing on the horizontal and vertical distribution  
50 of the Ocean Heat Content (OHC) and on the availability of Argo float profiles, five study areas that are most affected by warming and have high data coverage, were selected for our analysis.



Product ref. no.	Product ID & type	Data access	Documentation
1	INSITU_MED_PHYBGCWAV_DISCRETE_MYNRT_013_035; In-situ observations	EU Copernicus Marine Service Product, 2022a;	Quality Information Document (QUID): Wehde et al., (2022) Product User Manual (PUM): In Situ TAC partners (2022)
2	MEDSEA_MULTIYEAR_PHY_006_004; numerical models	EU Copernicus Marine Service Product, 2022b;	Quality Information Document (QUID): Escudier al., (2022) Product User Manual (PUM): Lecci et al., (2022)
3	SEALEVEL_EUR_PHY_L4_NRT_OBSERVATIONS_008_060; satellite observations	EU Copernicus Marine Service Product, 2023;	Quality Information Document (QUID): Pujol al., (2023) Product User Manual (PUM): Pujol., (2022a)
4	SEADATANET_MedSea_climatology_V2; climatology	SEADATANET Product; 2022	Product Information Document (PIDoc): Simoncelli et al. (2020)

**Table 1: Product data used to perform the analysis of the present work**



60

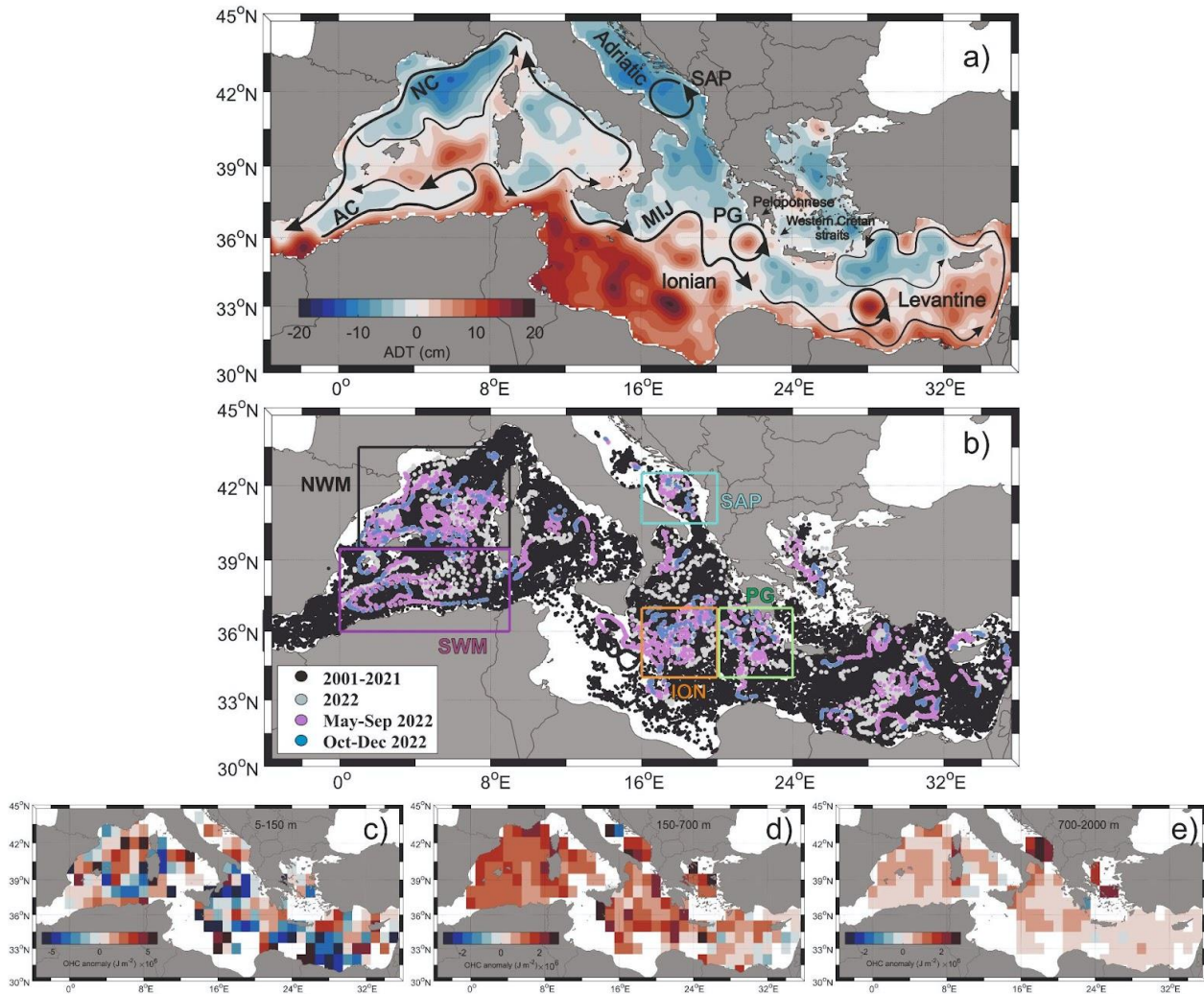


**Figure1:** (a) Absolute Dynamic Topography (colours) averaged from spring-summer (May-September 2022) along with schematic pathways (black arrows) of the Algerian Current (AC), Northern Current (NC), Mid-Ionian Jet (MIJ), South Adriatic Pit (SAP) and Pelops Gyre (PG). (b) Argo floats position for the whole Mediterranean Sea. Black, magenta, cyan, orange and green boxes indicate the North West Mediterranean (NWM, 39.5-43.5°N; 1-9°E), South West Mediterranean (SWM, 36-39.5°N; 0-9°E), South Adriatic Pit (SAP, 40.5-42.5°N; 16-20°E), Ionian (ION, 34-37°N; 13-20°E) and Pelops Gyre (PG, 34-37°N; 20-24°E) areas, respectively. (c-e) 2022 Ocean Heat Content (OHC) anomaly estimated with respect to the 2001-2018 FLOAT climatology period from Argo floats profiles in different layers (c, 5-150m), (d, 150-700), (e, 700-2000).

Based on the vertical heat penetration (MHW depth, see Methods section), the temperature profiles collected during the event from each study area were divided into three categories (shallow, intermediate and deep penetration) and the mean profile of

70



temperature anomaly ( $T_a$ ) was computed for each of them. Changes of the vertical temperature anomalies were described and analysed in relation to the ocean stratification, circulation and dynamics of each specific area. Moreover, the analysis of the water column characteristics after the event, in relation to the heat storage and the vertical propagation of the MHWs occurred during the previous May-September period, is also part of the work.

## 75 **Methods**

The vertical propagation of the 2022 MHW in the Mediterranean Sea was investigated using temperature data collected by Argo floats in the period 2001-2022 (Figure 1(b)). These data were collected and made freely available by the International Argo Program and the national programs that contribute to it. (<https://argo.ucsd.edu>, last access 23 April 2023; <https://www.ocean-ops.org>, last access 23 April 2023). The Argo Program is part of the Global Ocean Observing System  
80 (Argo 2023).

A comprehensive characterization of the event over the whole Mediterranean Sea was performed starting from the OHC analysis. The OHC, defined as the total amount of heat absorbed and stored by the ocean, can be considered as a good indicator for assessing the Earth's energy imbalance (Von Schuckmann et al., 2016). A float derived OHC climatology ( $OHC_{2001-2018}$ ) for the period 2001-2018 was estimated in  $1^\circ \times 1^\circ$  bins and in different layers (0-150 m, 150-700 m, 700-2000 m) using the  
85 method of Kubin et al., 2023. Subsequently, Argo temperature data collected in 2022 were averaged on the same grid of  $OHC_{2001-2018}$  to compute the 2022 OHC ( $OHC_{2022}$ ). The  $OHC_{2022}$  was then calculated as the difference between  $OHC_{2022}$  and  $OHC_{2001-2018}$  fields, and was used to select the five Mediterranean Sea regions most affected by warming in different layers and better sampled by floats (Figure 1b): the North Western Mediterranean (NWM), the South Western Mediterranean (SWM), the Ionian (ION), the Southern Adriatic Pit (SAP) and the Pelops Gyre (PG) sectors.

90 The  $T_a$  at each depth  $z$  and for each profile was computed as:

$$T_a(z) = T(z) - \bar{T}(z), \quad (1)$$

for each sector.  $T(z)$  is the 2022 temperature derived from Argo floats while  $\bar{T}(z)$  is the climatological (1985-2018) averaged temperature derived from the SeaDataCloud dataset (Product ref. no. 4, Table 1; SDC climatology). Specifically, the gridded ( $0.125^\circ \times 0.125^\circ$ ) monthly climatological profiles were linearly interpolated in depth and at the position of each float profile. Moreover, to compare the 2022 MHW event with the averaged conditions estimated by floats in the selected sectors,  $T_a$  profiles  
95 were also computed for the whole float dataset in the period 2001-2018 (FLOAT climatology).

The time window used for the present work (May-September 2022) was chosen based on the latest European Space Agency specification ([https://www.esa.int/Applications/Observing\\_the\\_Earth/Mediterranean\\_Sea\\_hit\\_by\\_marine\\_heatwave](https://www.esa.int/Applications/Observing_the_Earth/Mediterranean_Sea_hit_by_marine_heatwave), last access 18 February 2023). This indicates that the 2022 MHW developed in the second half of April in the northwest



100 Mediterranean Sea and extended over the central Mediterranean into September. In this period,  $T_a$  profiles were quality controlled to remove any inconsistency (e.g. profiles with negative surface anomalies) and used to estimate the vertical propagation of the MHW (or MHW depth), following the method of Elzahaby and Schaeffer 2019. For each profile, the positive threshold depth (hereafter  $Z_N$ ) is defined as the depth at which the first negative or 0 temperature anomaly occurred:

$$Z_N = \min(z(T(z) \leq 0)) , \quad (2)$$

Knowing  $Z_N$ , the vertical cumulative temperature anomaly ( $CT_a$ ) defined as:

$$CT_a(Z_N) = \sum_{z=0}^{Z_N} T(z) \Delta z , \quad (3)$$

105 with  $\Delta z = 10$  m, was computed for each profile from the surface ( $z=0$ ) to the positive threshold depth ( $z=Z_N$ ). To reduce the effect of the insignificant warming at depths per water profile, we define the MHW depth as the depth where a fraction ( $\varepsilon=0.95$ ) of the cumulative  $T_a$  is reached:

$$MHWdepth = \max\left(z\left(CT_a(z) \leq \varepsilon \cdot CT_a(Z_N)\right)\right) , \quad (4)$$

Based on MHW depth values,  $T_a$  profiles were then divided into three categories: Category 1 (shallow, 0-150 m), Category 2 (intermediate, 150-700 m) and Category 3 (deep, > 700 m). The mean  $T_a$  profile ( $\bar{T}_a$ ) for each category was obtained spatially averaging all the available data in the different sectors in the spring-summer period using both 2022 and FLOAT climatology  
110 Argo data. To understand how the heat accumulated in the water column during the MHW occurrence was distributed throughout it after the event, the averaged fall (October-December)  $\bar{T}_a$  profiles were also analysed. The mean  $\bar{T}_a$  averaged in the surface, intermediate and deep layers as well as other additional information (number of profiles, MHW depth, max  $T_a$  and depth of max) are listed in Table 2.

115 Lastly, the Brunt-Väisälä frequency squared ( $N^2$ ) for the year 2022 and in the upper 150 m depth was computed using monthly averaged temperature and salinity Argo floats profiles for each sector. The same procedure was adopted to calculate the  $N^2$  anomaly with respect to FLOAT climatology.



			Number of profiles	MHW depth (m)	T anomaly (°C)			Mean T anomaly (°C)		
					at the surface (10 m)	Max	Depth of Max (m)	0-150 m	150-700 m	700- 2000 m
NWM	spring summer	C1	335	24.8	2.3	5.82	22.5	0.28	0.32	0.097
		C2	16	571.9	2.2	5.48	50	0.32	0.4	NaN
		C3	43	1457.9	2.92	5.58	19.5	0.8	0.36	0.1
		clim	2460	-	-	-	-	0.12	0.06	0.025
	fall	2022	306	-	-	-	-	0.66	0.33	0.11
		clim	1284	-	-	-	-	0.08	0.07	0.04
SWM	spring summer	C1	159	25.6	2.13	5.79	22.5	0.19	0.33	0.088
		C2	5	630	1.83	5.46	24	0.43	0.3	NaN
		C3	27	1409.6	2.24	5.05	24.1	0.86	0.36	0.095
		clim	2168	-	-	-	-	0.028	0.059	0.028
	fall	2022	148	-	-	-	-	0.18	0.31	0.11
		clim	1456	-	-	-	-	0.1	0.05	0.02
ION	spring summer	C1	105	22.8	1.34	4.58	22.2	0.03	0.27	0.12
		C2	5	644	2.18	2.87	18	0.58	0.35	0.54
		C3	3	1383.4	1.39	1.97	20	0.47	0.54	0.15
		clim	1148	-	-	-	-	0.071	0.091	0.057
	fall	2022	119	-	-	-	-	-0.21	0.26	0.12
		clim	695	-	-	-	-	-0.06	0.07	0.05
PG	spring summer	C1	50	37	1.34	3.82	41	0.15	0.32	0.03
		C2	15	553.4	0.95	6.15	47.3	0.97	0.34	0
		C3	20	1043.5	0.88	5.34	40	1.14	0.58	0.05
		clim	1073	-	-	-	-	0.3	0.15	0.02
	fall	2022	70	-	-	-	-	-0.2	0.19	-0.02
		clim	590	-	-	-	-	0.27	0.13	0
SAP	spring summer	C1	9	32.2	1.18	3	24.5	0.57	0.39	0.66
		C2	10	411	1.95	7.25	27	1.04	0.46	NaN
		C3	17	945.3	0.88	4.36	78.8	0.72	0.4	0.59
		clim	619	-	-	-	-	0.3	0.21	0.21
	fall	2022	44	-	-	-	-	0.27	0.41	0.69
		clim	372	-	-	-	-	0.29	0.2	0.16

Table 2: Characteristics of the 2022 MHW in Category 1(C1), Category 2 (C2), Category 3 (C3): MHW depth, surface temperature anomaly (Surface), maximum temperature anomaly (Max) and the depth where it occurs (Depth of max), mean temperature anomaly for the surface (0-150 m), intermediate (150-700 m) and deep (700-2000 m) layers for each category and for the FLOAT Climatology (clim).

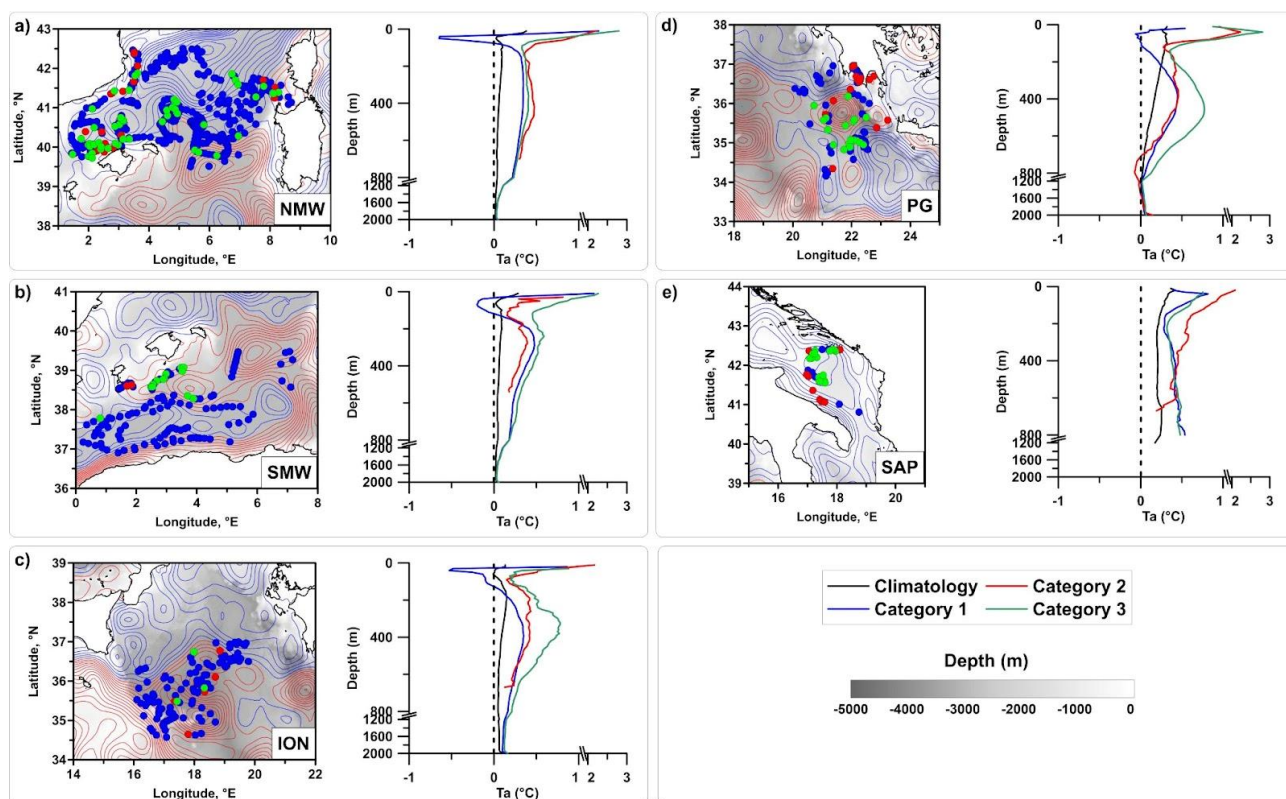
120



## Results and discussion

In the surface layer, the OHCA<sub>2022</sub> displayed inhomogeneous warming patterns, with positive anomalies areas adjacent to others with strong negative anomalies (Figure 1(c)). Warming was more homogeneous and widespread in the intermediate and deep layers (Figures 1(d), 1(e)) where the majority of bins showed positive values of the OHCA<sub>2022</sub>. The western and central Mediterranean areas along with the Aegean Sea showed a more pronounced warming compared to the Levantine basin which exhibits a slight cooling in some bins of the central and eastern sectors.

To perform this study, five regions (NWM, SWM, ION, SAP and PG; coloured boxes in Figure 1(b)) were selected as a compromise between the highest OHCA<sub>2022</sub> values and the availability of float data in both May-September (spring-summer) and October-December (fall) 2022 periods. Figure 2 shows  $\bar{T}a$  profiles in each sector for each MHW depth category and for the FLOAT climatology. In the NWM and SWM sectors, float profiles were located along the boundary of cyclonic circuits as highlighted by the Absolute Dynamic Topography (Product ref. no. 3, Table 1; (Figures 2(a), 2(b))).



135 **Figure 2: Temperature anomaly profiles computed for each sector (NWM, SWM, ION, PG, SAP) and from spring-summer (May-September 2022) Argo floats data with respect to the 1985-2018 SDC climatology dataset. Black lines highlight the FLOAT climatology profiles while blue, red and green profiles (dots) indicate shallow (0-150 m), intermediate (150-700 m) and deep (> 700m)**





categories, respectively. Positive and negative contours of the Absolute Dynamic Topography with 1 cm spacing are displayed by red and blue lines.

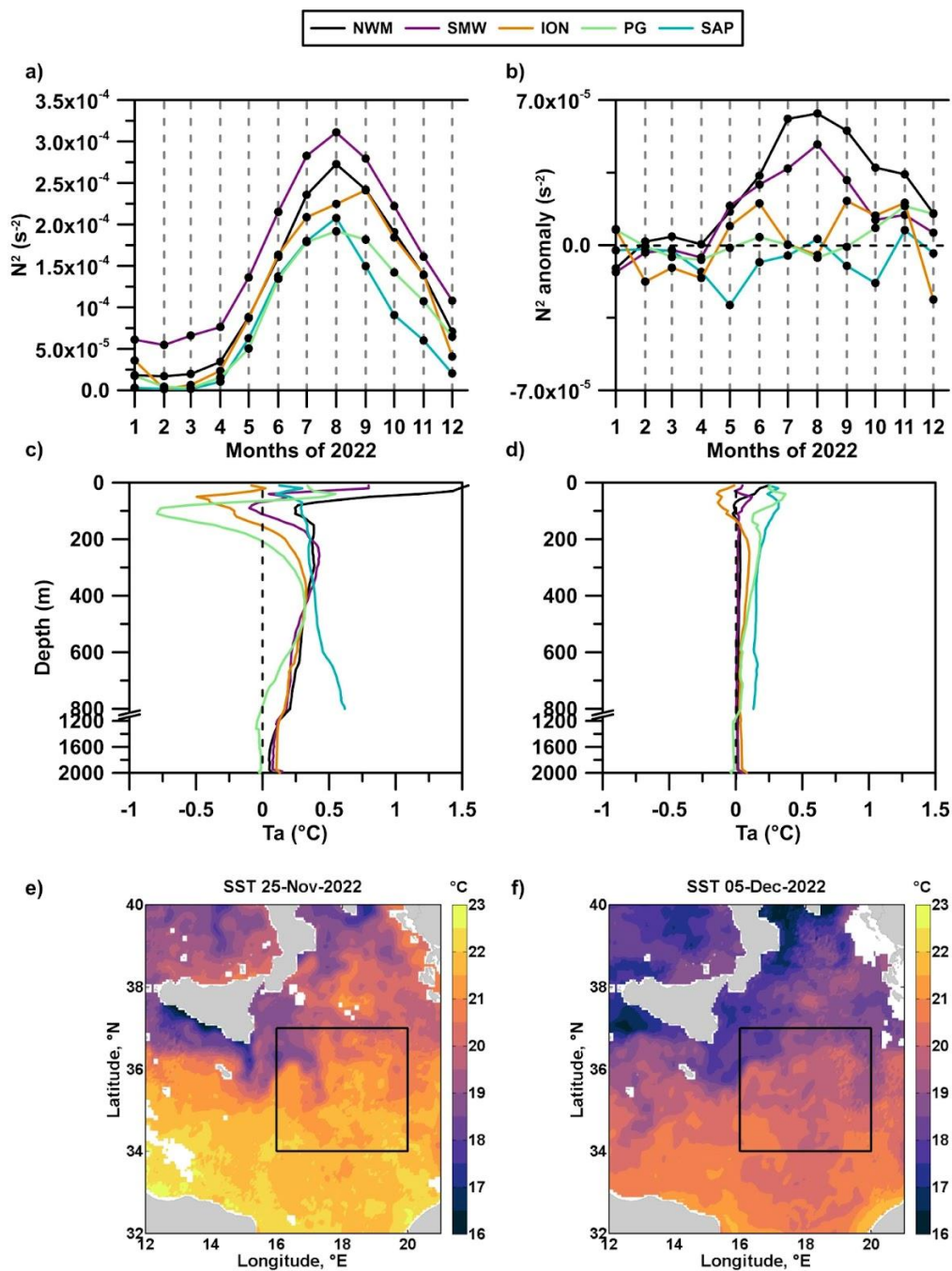
140 The circulation in these regions is strongly influenced by the presence of two intense and permanent currents (Figure 1(a)): the south-westward Northern Current in the NWM (Poulain et al., 2012; Escudier et al., 2021) and the strong eastward along-slope Algerian Current in the SWM, which transports waters of Atlantic origin in the upper water column (Poulain et al., 2021). In the ION sector, float profiles were mainly located in the anticyclonic meander of the Mid-Ionian Jet (Figure 2(c)), a strong meandering current that together with the Atlantic-Ionian Stream (AIS), transports Atlantic Water from the western to the eastern Mediterranean Sea (Poulain et al., 2012, 2013; Menna et al., 2019a; Figure 1(a)). Although the NWM, SWM and ION sectors have different oceanographic characteristics, they showed a similar response to the 2022 MHW (Figure 2(a-c)). Most  $\bar{T}a$  profiles belong to Category 1 and the mean MHW depth falls into the 20-25 m layer (Table 2). Profiles, characterized by shallow MHW penetration (blue lines in Figures 2(a-c)), showed decreasing warming in the first 50 m with the maximum  $\bar{T}a$  close to the surface (22.2-22.5 m; Table 2). The layer between 50 and 100 m depth showed a negative  $\bar{T}a$  with maxima of -0.65° C, -0.2° C and -0.53° C at 50 m, 70 m and 40 m depth, in the NWM, SWM and ION sectors, respectively. The mean profiles derived from the FLOAT climatology (black lines in Figure 2(a-c)) clearly do not exhibit this negative anomaly suggesting, therefore, a possible link between this behaviour and the occurrence of the 2022 MHW. Below 100 m depth, the  $\bar{T}a$  becomes positive again with mean values of ~ 0.3° C in the intermediate layer and values lower than 0.12° C in the deep layer. Profiles characterised by intermediate MHW penetration (red lines in Figures 2(a-c); MHW depth between 570 m and 650 m, Table 2) were located in coastal areas of the Western Mediterranean and in frontal zones in the ION sector, and showed positive  $\bar{T}a$  throughout the water column, with values in the range of 0.3 - 0.6° C. Profiles, characterised by deep MHW penetration (green lines in Figures 2(a-c); MHW depth ~ 1400 m, Table 2), showed the largest  $\bar{T}a$  in the surface layer in the two sectors of the West Mediterranean (> 0.8° C), while the ION sector depicted the largest anomalies in the intermediate layer (> 0.5° C). These results are consistent with the warming trend of the Western Mediterranean Sea over the last 15 years of 0.09±0.02 (0.03±0.01)° C·yr<sup>-1</sup> for surface (intermediate) waters (Kubin et al., 2023).

The PG is located on the eastern side of the northern Ionian Sea, southwest of the Peloponnese coast (Figure 1(a)). It is a sub-basin anticyclonic feature (diameter of ~120 km; Pinardi et al., 2015) which extends from the surface down to 800-1000 m depth (Malanotte-Rizzoli et al., 1997; Kovacevic et al., 2015) and it is forced by the Etesian winds (Ayoub et al., 1998; Mkhinini et al., 2014; Menna et al., 2021). In the late summer/fall the Etesian winds amplify their acceleration and the wind shear in the region of the western Cretan straits (Mkhinini et al., 2014) therefore, larger anticyclonic vorticities are observed during these months in the surface layer of the PG region (Menna et al., 2019a). In the sector PG,  $\bar{T}a$  profiles for the three categories showed positive temperature anomalies in the first 800 m of the water column which coincides with the vertical extension of the gyre itself (Figure 2(d)). Profiles that fall into Category 1 showed decreasing warming in the first 50 m, anomaly values close to zero in the 50-100 m layer and increasing warming in the 100-400 m layer. The mean anomaly in the intermediate layer of Category 1 is 0.3°C (Table 2). Category 2 profiles were retrieved mainly in the coastal area near the



Peloponnese while Category 3 profiles were found within the gyre area. Categories 2 and 3 showed strong warming in the surface layer ( $0.97^{\circ}\text{C}$  and  $1.14^{\circ}\text{C}$ , respectively), a mean warming in the range of  $0.3\text{-}0.6^{\circ}\text{C}$  in the intermediate layer and no warming compared to the SDC climatology was observed in the deep layer (Table 2).

175 The SAP is one of the sites of open ocean convection in the Mediterranean Sea, characterised by a complex thermohaline  
circulation that influences the physical and biogeochemical properties of the dense waters formed in its interior and the strength  
of winter convection (Menna et al., 2022 OSR6; Pirro et al., 2022). This sector showed positive temperature anomalies in all  
layers and in all categories (Figure 2(d)). Most profiles belong to Category 3 with a mean MHW depth of  $\sim 950\text{ m}$  and  
maximum  $T_a$  at  $\sim 80\text{ m}$  depth. The largest mean warming was observed in the surface layer of each category ( $0.6\text{-}1.4^{\circ}\text{C}$ )  
followed by the deep layer, which had an exceptional warming of  $\sim 0.6^{\circ}\text{C}$ , and finally by the intermediate layer, with a mean  
180 warming of  $\sim 0.4^{\circ}\text{C}$  (Table 2). All five sectors showed a larger warming than the FLOAT climatology with temperature  
increases in spring-summer 2022 between  $0.2^{\circ}\text{C}$  and  $0.8^{\circ}\text{C}$  in response to the MHW event (Table 2). Some differences in  
warming observed among the sectors are related to their peculiar hydrological and dynamical characteristics. During the  
spring-summer period, the surface layer of the NWM and SWM sectors and partially of the ION sector, was characterised by  
both larger stratifications and stratification anomalies compared to the FLOAT climatology (Figures 3(a), 3(b)). Strong  
185 stratification prevents vertical heat penetration causing negative  $T_a$  in the  $50\text{-}100\text{ m}$  layer (Figure 2(a-c)). In the PG sector,  
summer-spring stratification was consistent with climatology (Figure 3(b)), and vertical heat penetration was closely related  
to the gyre dynamics. In the SAP sector, stratification during the summer-spring period was lower than climatology; this  
suggests an instability of the water column and therefore the transport of the vertical heat to the deep layers.



190 **Figure3:** (a) Monthly averaged Brunt - Väisälä frequency squared ( $N^2$ ) computed in the surface layer (0-150 m) using 2022 Argo float data. (b) Monthly averaged Brunt Brunt—Väisälä frequency squared anomaly ( $N^2$  anomaly) computed in the surface layer with respect to the FLOAT climatology. (c) Mean Temperature anomaly ( $^{\circ}\text{C}$ ) computed in fall period (October - December) from



**Argo floats profiles in 2022 and (d) in 2001-2018 with respect to the SDC climatology). (e) Daily Sea Surface Temperature (°C) in the ION sector (black box) between November and (f) December 2022.**

195 Larger warming of the water column was observed in fall 2022 compared to the SDC climatology in all sectors, except for the surface layer of the two sectors located in the Ionian Sea (ION and PG). The stronger spring-summer stratification observed in the NWM and SWM sectors (Figures 3(a), 3(b)) corresponds to enhanced vertical heat propagation in the surface and intermediate layers in fall 2022 (Figure 3(c), Table 2). Negative  $T_a$  values in the surface layer of the ION sector were attributed to an upwelling event along the southern coast of Sicily between November and December 2022 as shown by the Sea Surface  
200 Temperature (Product ref. no. 2, Table 1; (Figures 3(e), 3(f)). The northern part of the Sicily Channel is an area of strong eddy kinetic energy (Poulain et al., 2012) influenced by Ekman transport and advection of waters from the western to the eastern Mediterranean (Molcard et al., 2002; Falcini et al., 2015; Schroeder et al., 2017; Menna et al., 2019b). The cold waters upwelled off the southern coast of Sicily in November 2022 (Figure 3(e)) were advected to the Ionian Sea through the Atlantic-Ionian Stream and the Mid-Ionian Jet pathways (Figure 1(a)), and gradually cooling the waters in the ION sector (Figure 3(f)). The  
205 negative anomaly in the surface layer of the ION sector is not limited only to 2022 but is a permanent characteristic of the area related to the upwelling phenomena, as confirmed by the  $\bar{T}_a$  profile derived from the FLOAT climatology (orange line in Figure 3(d)) and by trends of the OHC anomaly estimated by Dayan et al. (2023) over the period 1987-2019. Negative  $\bar{T}_a$  values in the PG sector were imputable to the typical downwelling process of this region associated with the gyre dynamics. The downwelling contributed to the vertical propagation of the 2022 MHW, with a strong spring-summer warming in the first  
210 800 m of the water column (Figure 2d), keeping the stratification values similar to the FLOAT climatology (no significant increases of  $N^2$  anomaly was registered due to the 2022 heatwave; Figure 3(b)). In this way, fall cooling can penetrate deep into the water column causing, therefore, negative  $T_a$  values in the surface layer (Figure 3(c); Table 2).

In recent years, the SAP is experiencing a significant temperature increase in the deep layer (trend of  $\sim 0.06^\circ \text{C}\cdot\text{yr}^{-1}$  in the 2013-2020 period according to Kubin et al., 2023) and salinity in the surface and intermediate layers (Mihanovich et al., 2021; Menna et al., 2022 OSR6) with potential future effects on the whole thermohaline cell of the Eastern Mediterranean. It is of general understanding that convection sites contribute to the propagation of the MHWs signal from the surface to the subsurface interior of the water column (Dayan et al., 2023; Kubin et al., 2023) but specific analysis at the local scale are not yet available (Juza et al., 2022). Our results show a fair significant warming of the SAP in both spring summer (Figure 2(e)) and fall (light blue line in Figure 3(c)) 2022 and a significant positive anomaly of FLOAT climatology compared to SDC one  
220 (black line in Figure 2(e) and light blue line in Figure 3(d)). In fall, largest  $\bar{T}_a$  in the SAP were observed in the deep layer ( $\sim 0.69^\circ \text{C}$ ); Table 2, Figure 3(c)). Mean profiles derived from Float Climatology (black line in Figure 2(e) and light blue line in Figure 3(d)) showed positive values compared to SDC one, confirming the warming trend throughout the water column over the past decade. Beyond the impact of the global warming of the Mediterranean Sea, the 2022 MHW leads to an additional heating in the SAP, which is transferred to the deeper layers favoured by dynamical features of this area.



225 This study shows that the effects of the 2022 MHW are felt in all layers of the Mediterranean Sea with vertical heat propagation  
extending from the surface to ~1500 m depth. In the surface layer, heat penetration and storage are related to the strength of  
the stratification and/or advection from adjacent regions. In contrast, the transport and the storage of heat in the intermediate  
and deep layers are closely linked to the dynamics of each area. In the western Mediterranean and western Ionian Sea sectors,  
heat is mainly stored in the surface layer (shallow MHW depths and stronger stratification) so that this layer is significantly  
230 warmer than the climatology even during the following fall. Although deep MHW penetration in these regions is limited to  
coastal and frontal/eddies zones, it reaches the higher MHW depth estimated during the event. Sectors characterised by specific  
dynamics conditions (downwelling, convection) quickly distribute the heat in the water column even during the event.  
Intermediate layers show similar heating both during and after the MHW event, suggesting that heat can be stored here for  
long periods. The warming signal in the intermediate and deep layers could also be influenced by heat advection from adjacent  
235 basins however, we are aware that this topic needs to be studied in more detail in the future. In this context, the use of two  
climatologies and the cumulative anomaly threshold in the present analysis should have eliminated most of the signal  
associated with the ocean warming trend and advection. In conclusion, it is a matter of fact that the additional warming  
registered in spring-summer 2022 compared to the FLOAT climatology can be attributed to the effects of the 2022 MHW  
along the entire water column. This sheds light on possible scenarios changes with implications on the variation of the ocean  
240 processes that regulate the thermohaline circulation and thus, the climate system.



Competing interests. The contact author has declared that neither they nor their co-authors have any competing interests.

245

Author contributions. Conceptualization of the study was done by AP, MM and RM. AP and MM prepared the original manuscript. AP, MM, RM, EM, AG, GN, EK and MJ reviewed and edited the manuscript. AP, MM and RM created the methodology. AP, MM, RM and EK created the codes and performed the formal analysis. AP, MM, RM conducted the investigation. AG, AB and MP curated the data. EM was in charge of Argo-Italy infrastructure management and funding acquisition. All authors have read and agreed to the published version of the paper.

250

## References

- Argo: Argo float data and metadata from Global Data Assembly Centre (Argo GDAC). SEANOE. <https://doi.org/10.17882/42182>, 2023.
- Ayoub, N., Le Traon, P.-Y., and De Mey, P.: A description of the Mediterranean surface variable circulation from combined ERS-1 and TOPEX/POSEIDON altimetric data, *J.Mar. Syst.* 18, 3–40, doi: 10.1016/S0924-7963(98)80004-3, 1998.
- Bensoussan, N., Chiggiato, J., Buongiorno Nardelli, B., Pisano, A. and Garrabou, J.: Insights on 2017 marine heat waves in the Mediterranean sea, *J. Oper. Ocean.*, 12 (1), s26–s30. doi:10.1080/1755876X.2019.163307, 2019.
- Darmaraki, S., Somot, S., Sevault, F. and Nabat, P.: Past variability of Mediterranean Sea marine heatwaves, *Geophys. Res. Lett.*, 46 (16), 9813–9823, doi: 10.1029/2019GL082933, 2019.
- 260 Dayan, H., McAdam, R., Juza, M., Masina, S. and Speich, S.: Marine heat waves in the Mediterranean Sea: An assessment from the surface to the subsurface to meet national needs. *Front. Mar. Sci.*, 10:1045138, doi: 10.3389/fmars.2023.1045138, 2023.
- Elzahaby, Y. and Schaffer, A.: Observational insight into the subsurface anomalies of marine heatwaves, *Front. Mar. Sci.*, 6:745, doi: 10.3389/fmars.2019.00745, 2019.
- 265 Escudier, R., Clementi, E., Cipollone, A., Pistoia, J., Drudi, M., Grandi, A., Lyubartsev, V., Lecci, R., Aydogdu, A., Delrosso, D., Omar, M., Masina, S., Coppini, G. and Pinardi, N.: A High Resolution Reanalysis for the Mediterranean Sea, *Front. Earth Sci.* 9:702285, doi: 10.3389/feart.2021.702285, 2021.
- Falcini, F. and Salusti, E.: Friction and mixing effects on potential vorticity for bottom current crossing a marine strait: an application to the Sicily Channel (central Mediterranean Sea), *Ocean Sci.*, 11, 391–403, doi:10.5194/os-11-391-2015, 2015.
- 270 Galli, G., Solidoro C., and Lovato T.: Marine heat waves hazard 3D maps and the risk for low motility organisms in a warming Mediterranean Sea, *Frontiers in Marine Science* 4: 136, 2017.
- Garrabou, J. et al.: Marine heatwaves drive recurrent mass mortalities in the Mediterranean Sea. *Global Change Biology*, 2022
- Hobday, A. J., Alexander, L. V., Perkins, S. E., Smale, D. A., Straub, S. C., Oliver, E. C., Benthuisen, J. A., Burrows, M. T., Donat, G. M., Feng, M., Holbrook, N., J., Moore, P. J., Scannel, H. A., Gupta, A. S. and Wernberg T.: A hierarchical approach to defining marine heatwaves, *Prog. Oceanogr.* 141, 227–238, doi: 10.1016/j.pocean.2015.12.014, 2016.
- 275 Ibrahim, O., Mohamed, B., and Nagy, H.: Spatial variability and trends of marine heat waves in the Eastern Mediterranean Sea over 39 years, *J. Mar. Sci. Eng.* 9 (6), 643, doi: 10.3390/jmse9060643, 2021.



- 280 Intergovernmental Panel on Climate Change (IPCC): Summary for Policymakers. In: Climate Change 2023, Synthesis Report, Summary for Policymakers, Core Writing Team, Lee, H. and Romero, J., 36, [https://www.ipcc.ch/report/ar6/syr/downloads/report/IPCC\\_AR6\\_SYR\\_SPM.pdf](https://www.ipcc.ch/report/ar6/syr/downloads/report/IPCC_AR6_SYR_SPM.pdf), 2023.
- Juza, M., Fernández-Mora, A., and Tintoré, J.: Sub-Regional marine heat waves in the Mediterranean Sea from observations: long-term surface changes, subsurface and coastal responses, *Front. Mar. Sci.* 9, 785771, doi: 10.3389/fmars.2022.785771, 2022.
- 285 Kovačević, V., Ursella, L., Gačić, M., Notarstefano, G., Menna, M., Bensi, M., and Poulain, P.-M.: On the Ionian thermohaline properties and circulation in 2010-2013 as measured by Argo floats, *ACTA ADRIAT.*, 56(1): 97 - 114, 2015.
- Kubin, E., Menna, M., Mauri, E., Notarstefano, G., Mieruch, S., and Poulain, P.-M.: Heat content and temperature trends in the Mediterranean Sea as derived from Argo float data, *Front. Mar. Sci.* (submitted to *Frontiers*), 2023
- 290 Malanotte-Rizzoli, P., Manca, B. B., Ribera D'Alcalà, M., Theocharis, A., Bergamasco, A., Bregant, D., Budillon, G., Civitarese, G., Georgopoulos, D., Michelato A., Sansone, E., Scarazzato, P., Souvermezoglou, E.: A synthesis of the Ionian Sea hydrography, circulation and water masses pathways during POEM-Phase I, *Progr. Oceanogr.*, 39, 153–204, [https://doi.org/10.1016/S0079-6611\(97\)00013-X](https://doi.org/10.1016/S0079-6611(97)00013-X), 1997.
- Menna, M., Suarez, N. R., Civitarese, G., Gačić, M., Rubino, A., and Poulain, P. M.: Decadal variations of circulation in the Central Mediterranean and its interactions with mesoscale gyres, *Deep Sea Res. II*, 164, 14-24, <https://doi.org/10.1016/j.dsr2.2019.02.004>, 2019a.
- 295 Menna, M., Poulain, P. M., Ciani, D., Doglioli, A., Notarstefano, G., Gerin, R., Rio, M. H. Santoleri, R., Gauci, A. and Drago, A.: New Insights of the Sicily Channel and Southern Tyrrhenian Sea Variability, *Water*, 11, 1355, 10.3390/w11071355, 2019b.
- Menna, M., Gerin, R., Notarstefano, G., Mauri, E., Bussani, A., Pacciaroni, M., and Poulain, P. M.: On the circulation and thermohaline properties of the Eastern Mediterranean Sea, *Fron. Mar. Sci.*, 8, 671469, <https://doi.org/10.3389/fmars.2021.6714692>, 2021.
- 300 Menna, M., Martellucci, R., Notarstefano, G., Mauri, E., Gerin, R., Pacciaroni, M., Bussani, A., Pirro, A., Poulain, P. M.: Record-breaking high salinity in the South Adriatic Pit in 2020, *J. Oper. Oceanogr.*, s199-s205, <https://doi.org/10.1080/1755876X.2022.2095169>, 2022.
- Mihanović, H., Vilibić, I., Šepić, J., Matić, F., Ljubešić, Z., Mauri, E., Gerin, R.: Observation, preconditioning and recurrence of exceptionally high salinities in the Adriatic Sea, *Front. Mar. Sci.*, 8:834. doi:10.3389/fmars.2021.672210, 2021.
- 305 Molcard, A., Gervasio, L., Gria, A., Gasparini, G. P., Mortier, L., Ozgokmen, T. M.: Numerical investigation of the Sicily Channel dynamics: density currents and water mass advection. *J. Mar. Syst.*, 36, 219–238, [https://doi.org/10.1016/S0924-7963\(02\)00188-4](https://doi.org/10.1016/S0924-7963(02)00188-4), 2002.
- Mkhinini, N., Coimbra, A. L. S., Stegner, A., Arsouze, T., Taupier-Letage, I., and Beranger, K.: Long-lived mesoscale eddies in the Eastern Mediterranean Sea: analysis of 20 years of AVISO geostrophic velocities, *J. Geophys. Res. Oceans* 119, 8603–8626, doi: 10.1002/2014JC010176, 2014.
- 310 Oliver, E. C., Donat, M. G., Burrows, M. T., Moore, P. J., Smale, D. A., Alexander, L. V., Benthuisen, J. A., Feng, M., Gupta, A. S., Hobday, A. J., Holbrook, N. J., Perkins-Kirkpatrick, S. E., Scannell, H. E., Straub, S. C. and Wernberg, T.: Longer and more frequent marine heatwaves over the past century, *Nat. Commun.*, 9:1324, doi: 10.1038/s41467-018-03732-9, 2018.



- 315 Pinardi, N., Zavatarelli, M., Adani, M., Coppini, G., Fratianni, C., Oddo, P., Simoncelli, S., Tonani, M., Lyubartsev, V.: Mediterranean Sea large-scale low-frequency ocean variability and water mass formation rates from 1987 to 2007: a retrospective analysis, *Prog. Oceanogr.* 132, 318–332, doi: 10.1016/j.pocean.2013.11.003, 2015.
- Pirro, A., Mauri, E., Gerin, R., Martellucci, R., Zuppelli, P. and Poulain, P. M.: New insights on the formation and breaking mechanism of convective cyclonic cones in the South Adriatic Pit during winter 2018, *J. Phys. Oceanogr.*, 52(9), 2049–2068, <https://doi.org/10.1175/JPO-D-21-0108.1>, 2022.
- 320 Poulain, P. M., Menna, M., and Mauri, E.: Surface geostrophic circulation of the Mediterranean Sea derived from drifter and satellite altimeter data, *J. Phys. Oceanogr.*, 42(6), 973–990, <https://doi.org/10.1175/JPO-D-11-0159.1>, 2012.
- Poulain, P. M., Bussani, A., Gerin, R., Jungwirth, R., Mauri, E., Menna, M. and Notarstefano, G.: Mediterranean surface currents measured with drifters: From basin to subinertial scales. *Oceanography* 26 (1), 38–47, <http://dx.doi.org/10.5670/oceanog.2013.03>, 2013.
- 325 Poulain, P. M., Centurioni, L., Özgökmen, T., Tarry, D., Pascual, A., Ruiz, S., Mauri, E., Menna, M. and Notarstefano, G.: On the structure and kinematics of an Algerian Eddy in the southwestern Mediterranean Sea, *Rem. Sens.*, 13(15), 3039, <https://doi.org/10.3390/rs13153039>, 2021.
- Pastor, F. and Khodayar, S.: Marine heat waves: Characterizing a major climate impact in the Mediterranean, *Sci. Tot. Env.*, 861, 160621. doi: 10.1016/j.scitotenv.2022.160621, 2022.
- 330 Scannell, H. A., Johnson, G. C., Thompson, L., Lyman, J. M., and Riser, S. C.: Subsurface evolution and persistence of marine heatwaves in the Northeast Pacific, *Geophys. Res. Lett.*, 47, e2020GL090548. <https://doi.org/10.1029/2020GL090548>, 2020.
- Schroeder, K., Chiggiato, J., Josey, S.A., Borghini, M., Aracri, S., Sparnocchia, S.: Rapid response to climate change in a marginal sea, *Sci. Rep.*, 7, 4065, <https://doi.org/10.1038/s41598-017-04455-5>, 2017.
- 335 Shijian H., S., Li, S., Zhang, Y., Guan, C., Du, Y., Feng, M., Anodo, K., Wang, F., Schiller, A. and Hu, D.: Observed strong subsurface marine heatwaves in the tropical western Pacific Ocean. *Env. Res. Lett.*, 16(10), 104024,16 104024 DOI 10.1088/1748-9326/ac26f2, 2021.
- Von Schuckmann, K., Palmer, M. D., Trenberth, K. E., Cazenave, A., Chambers, D., Champollion, N., Hansen, J., Josey, S. A., Loeb, N., Mathieu, P. P., Meyssignac, B. and Wild, M.: An imperative to monitor earth’s energy imbalance, *Nat. Clim. Change*, 6 (2), 138–144, doi:10.1038/nclimate2876, 2016.
- 340 Wernberg, T., Smale, D. A., Tuya, F., Thomsen, M. S., Langlois, T. J., De Bettignies, T., Bennet, S. and Rousseaux, C. S.: An extreme climatic event alters marine ecosystem structure in a global biodiversity hotspot, *Nat. Clim. Change*, 3, 78–82, <https://doi.org/10.1038/nclimate1627>, 2013.
- 345 Wong, A. P., Wijffels, S. E., Riser, S. C., Pouliquen, S., Hosoda, S., Roemmich, D., et al.: Argo Data 1999–2019: Two Million Temperature-Salinity Profiles and Subsurface Velocity Observations From a Global Array of Profiling Floats, *Front. Mar. Sci.*, 7(700), doi: <https://doi.org/10.3389/fmars.2020.00700>, 2020.





## 350 **References for Table 1**

### Product ref no.1

EU Copernicus Marine Service Product: Mediterranean Sea- In-Situ Near Real Time Observations, Mercator Ocean International [data set], <https://doi.org/10.48670/moi-00044>, 2022.

355 H. Wehde, K. V. Schuckmann, S. Pouliquen, A. Grouazel, T Bartolome, J Tintore, M. De Alfonso Alonso-Munoyerro, T. Carval, V. Racapé and the INSTAC team: EU Copernicus Marine Service Quality Information Document for Mediterranean Sea- In-Situ Near Real Time Observations, INSITU\_MED\_PHYBGCWAV\_DISCRETE\_MYNRT\_013\_035, Issue 2.2, Mercator Ocean International, <https://catalogue.marine.copernicus.eu/documents/QUID/CMEMS-INS-QUID-013-030-036.pdf>, last access: 19 May 2023, 2022.

360 In Situ TAC partners: EU Copernicus Marine Service Product User Manual for Mediterranean Sea- In-Situ Near Real Time Observations, INSITU\_MED\_PHYBGCWAV\_DISCRETE\_MYNRT\_013\_035, Issue 1.14, Mercator Ocean International, <https://catalogue.marine.copernicus.eu/documents/PUM/CMEMS-INS-PUM-013-030-036.pdf>, last access: 19 May 2023, 2022.

### Product ref no.2

365 EU Copernicus Marine Service Product: Mediterranean Sea Physics Reanalysis, Mercator Ocean International [data set], [https://doi.org/10.25423/CMCC/MEDSEA\\_MULTIYEAR\\_PHY\\_006\\_004\\_E3R1I](https://doi.org/10.25423/CMCC/MEDSEA_MULTIYEAR_PHY_006_004_E3R1I), 2022.

R. Escudier, E. Clementi, T. Nigam, A. Aydogdu, E. Fini, J. Pistoia, A. Grandi, P. Miraglio: EU Copernicus Marine Service Quality Information Document for Mediterranean Sea Physics Reanalysis, MEDSEA\_MULTIYEAR\_PHY\_006\_004, Issue 2.3, Mercator Ocean International, <https://catalogue.marine.copernicus.eu/documents/QUID/CMEMS-MED-QUID-006-004.pdf>, last access: 19 May 2023, 2022.

370 Rita Lecci, Massimiliano Drudi, Alessandro Grandi, Sergio Creti, Emanuela Clementi: EU Copernicus Marine Service Product User Manual for For Mediterranean Sea Physics Reanalysis, MEDSEA\_MULTIYEAR\_PHY\_006\_004, Issue 2.3, Mercator Ocean International, <https://catalogue.marine.copernicus.eu/documents/PUM/CMEMS-MED-PUM-006-004.pdf>, last access: 19 May 2023, 2022.

### Product ref no.3

375 EU Copernicus Marine Service Product: European Seas Gridded L 4 Sea Surface Heights And Derived Variables Nrt, Mercator Ocean International [data set], <https://doi.org/10.48670/moi-00142>, 2023.

380 M-I Pujol, G. Taburet and SL-TAC team.: EU Copernicus Marine Service Quality Information Document for European Seas Gridded L 4 Sea Surface Heights And Derived Variables Nrt, SEALEVEL\_EUR\_PHY\_L4\_NRT\_OBSERVATIONS\_008\_060, Issue 8.2, Mercator Ocean International, <https://catalogue.marine.copernicus.eu/documents/QUID/CMEMS-SL-QUID-008-032-068.pdf>, last access: 19 May 2023, 2022.

385 M-I Pujol: EU Copernicus Marine Service Product User Manual for European Seas Gridded L 4 Sea Surface Heights And Derived Variables Nrt, SEALEVEL\_EUR\_PHY\_L4\_NRT\_OBSERVATIONS\_008\_060, Issue 7.0, Mercator Ocean International, <https://catalogue.marine.copernicus.eu/documents/PUM/CMEMS-SL-PUM-008-032-068.pdf>, last access: 19 May 2023, 2022.

### Product ref no.4

<https://doi.org/10.5194/sp-2023-14>  
Preprint. Discussion started: 19 September 2023  
© Author(s) 2023. CC BY 4.0 License.



S. Simoncelli , P. Oliveri , G. Mattia. SeaDataCloud Mediterranean Sea - V2 Temperature and Salinity Climatology [dataset].  
<http://dx.doi.org/10.12770/3f8eaace-9f9b-4b1b-a7a4-9c55270e205a> [Accessed on 19 May 2023]

390 Simoncelli Simona, Oliveri Paolo, Mattia Gelsomina, Myroshnychenko Volodymyr, Barth Alexander, Troupin Charles (2020).  
SeaDataCloud Temperature and Salinity Climatology for the Mediterranean Sea (Version 2). Product Information Document  
(PIDoc). <https://doi.org/10.13155/77514>